scientific reports

Check for updates

OPEN

Transcriptome enhanced rice grain metabolic model identifies histidine level as a marker for grain chalkiness

Niaz Bahar Chowdhury[1], Anil Kumar Nalini Chandran[2], Harkamal Walia[2] & Rajib Saha[1]✉

Rising temperatures due to global warming can negatively impact rice grain quality and yield. This study investigates the effects of increased warmer night temperatures (WNT), a consequence of global warming, on the quality of rice kernel, particularly grain chalkiness. By integrating computational and experimental approaches, we used a rice grain metabolic network to discover the metabolic factors of chalkiness. For this, we reconstructed the rice grain genome-scale metabolic model (GSM), iOSA3474-G and incorporated transcriptomics data from three different times of the day (dawn, dawn 7 h, and dusk) for both control and WNT conditions with iOSA3474-G. Three distinct growth phases: anoxia, normoxia, and hyperoxia, were identified in rice kernels from the GSMs, highlighting the grain-filling pattern under varying oxygen levels. We predicted excess flux through histidine contributing to the biomass as a marker of normoxia, during which kernel chalkiness occurs. Moreover, similarly, we proposed tyrosine as a marker for the hyperoxic growth phase. We also proposed a potential link between monodehydroascorbate reductase, an enzyme with evolutionary significance dating back to the carboniferous era, in regulating the hyperoxic growth phase. Metabolic bottleneck analysis identified nucleoside diphosphate kinase as a central regulator of metabolic flux under different conditions. These findings provide targeted insights into the complex metabolic network governing rice grain chalkiness under WNT conditions. Integration of GSM and transcriptomics data, enhanced our understanding of the intricate relationship between environmental factors, metabolic processes, and grain quality and also offer markers that can be useful to develop rice with improved resilience.

Keywords *Oryza sativa*, Chalkiness, Grain growth phases, Warmer night temperatures, Metabolic modeling.

Rice is a staple for more than half of the world's population, supplying over 21% of total caloric demands[1]. With projected increase in global population to 9 billion by 2050[2], the demand for rice will continue to rise sharply. However, global warming poses a significant challenge to meeting this demand. Predictions suggest a rise in global mean surface air temperatures of 1.0–3.7 °C by 2100[3], placing rice production cycle at heightened risk, particularly during grain filling, due to heat stress[4]. Recent studies also underscore the asymmetric increase in night-time temperatures compared to day-time temperatures[5,6], exerting an additional vulnerability to rice grain yield.

Exposure to warmer night-time (WNT) conditions during grain filling significantly reduces pollen viability, heightens spikelet sterility, compromises membrane integrity, and hinders grain growth, ultimately resulting in poor seed-set and reduced individual grain weight[7–9]. Changes in individual grain weight are often linked to limited carbohydrate supply[10] and alterations in starch metabolism enzymes[11]. Besides reduced grain yield, exposure to WNT also adversely affects grain quality, which often manifests as increased chalkiness[12]. Chalkiness is the opaque part of the grain found in an otherwise translucent white endosperm of rice. Chalk formation in rice grain arises from loosely packed starch granules, resulting in air spaces between amyloplasts[13], resulting in a higher proportion of broken grains and a significant decrease in the economic value of the rice[14].

Despite some understanding of rice grain chalkiness, further insights into its implications on the overall rice grain metabolism remains scarce. To address this, the development of a genome-scale metabolic model (GSM)[15,16] specific to rice grain, coupled with transcriptome data that potentially captures the increased chalkiness under

[1]Department of Chemical and Biomolecular Engineering, University of Nebraska-Lincoln, 1600 Vine Street, Lincoln, NE 68505, USA. [2]Department of Agronomy and Horticulture, University of Nebraska- Lincoln, 1600 Vine Street, Lincoln, NE 68505, USA. ✉email: rsaha2@unl.edu

WNT, could provide a novel insights into the role of metabolic perturbance under WNT. Previous successes in integrating transcriptomics data with GSMs have been demonstrated in predicting phenotypes, such as maize root phenotype under nitrogen starvation conditions and whole-plant phenotype of maize under heat and cold stress conditions[17,18]. Therefore, this approach holds promise for elucidating the metabolic pathways associated with rice grain chalkiness. While previous rice GSMs exist, they are consolidated whole-plant models and primarily focus on the photosynthetic apparatus under various conditions[19,20]. Although a multi-organ rice metabolic model has been developed recently[21], it lacks the resolution required to capture grain-related metabolism. Furthermore, only a limited studies have integrated relevant transcriptomics data with the models[20], a crucial process known as contextualization, essential for accurately predicting phenotypes[17]. Thus, the development of a grain-specific rice model, contextualized with a transcriptome response that is known to increase grain chalkiness under WNT stress, is essential for comprehensively understand the system-wide metabolic impacts of grain chalkiness.

To explore rice grain chalkiness, we constructed the first-ever rice grain GSM, iOSA3474-G, and contextualized it with a previously published WNT transcriptomics dataset[22] across three time points (dawn, dawn 7 h, and dusk) for both control and WNT conditions using the EXTREAM algorithm[18] that we have recently developed and accurately predicted the phenotype of maize plant under heat and cold stress conditions. Our analysis of contextualized GSMs revealed three distinct growth phases in rice grains: anoxia, normoxia, and hyperoxia. These phases shed light on grain-filling dynamics under varying oxygen levels. Notably, normoxia, characterized by low oxygen availability and warmer night temperatures, is closely associated with increased grain chalkiness. Notably, we predicted excess flux through histidine contributing to the biomass as a metabolic marker for normoxia, the phase coinciding with grain chalkiness occurrence, while excess flux through tyrosine contributing to the biomass as a metabolic marker for the hyperoxic growth phase. Furthermore, our investigation predicted the significant role of monodehydroascorbate reductase (MDAR)[23], an enzyme with evolutionary significance tracing back to the carboniferous era, in regulating the hyperoxic growth phase. Through metabolic bottleneck analysis, we proposed nucleoside diphosphate kinase as a central regulator of metabolic flux under both different conditions. These findings offer targeted insights into the intricate metabolic network governing rice grain chalkiness under WNT conditions. By integrating GSM and transcriptomics data, this approach not only advances our comprehension of the complex interplay between environmental factors, metabolic pathways, and crop quality but also presents practical avenues for enhancing crop resilience to global warming by perturbing the metabolic bottlenecks addressed in this study.

Results and discussion

Reconstruction of Genome-Scale metabolic model of rice grain

Maize, being a monocot, shares significant common ancestry with rice[24]. Comparative studies of Quantitative Trait Loci (QTL) between these two species have revealed that comparable traits are typically governed by QTLs located within syntenic regions[25]. Furthermore, genes influencing grain shape and weight in rice, such as GS5, have been demonstrated to regulate similar traits in maize[26,27]. Therefore, we choose to use our recently published maize kernel model[18] as a blueprint to reconstruct the rice grain model. Figure 1a shows the rice grain metabolic model reconstruction workflow.

Figure 1b shows the metabolic map of rice grain model. Overall, the model, iOSA3474-G, has 3474 genes, 4060 reactions, and 4474 metabolites (Fig. 1c) and is the most comprehensive rice grain metabolic model to date.

Next, rice grain biomass composition data was collected from the USDA website (Supplementary Data S1) and formulated in a way so that the molecular weight of biomass is 1 mmol/gDW[28]. Subsequently, for all the control and stress conditions, the same biomass equation was used. Additionally, for each biomass metabolite, we created a reaction in the model that transfers the metabolite from the cytosol to biomass. This approach allowed us to track the contribution of each biomass metabolite to the grain filling rates. Furthermore, in this work, biomass growth rate and grain filling rate was used interchangeably. Biomass composition comparison between maize kernel and rice grain revealed the difference in protein, lipid, fatty acids, and pigments compositions. The mole percentage of carbohydrate in rice is higher than the maize kernel (Fig. 1d). Interestingly, amino acid composition in rice grain is also higher than the maize kernel. Contrastingly, lipid content is maize is higher (3.41%) in maize kernel compared to the rice grain (0.24%).

One of the key differences between maize kernel and rice grain is its inability to produce pigments, without genetic perturbations[29]. Contrary to that, β-carotene and zeaxanthin are the major pigments in the maize kernel[30]. Interestingly, despite flux variability analysis showing reactions able to produce those pigments are able to carry fluxes, iOSA3474-G predicted no flux through β-carotene and zeaxanthin biosynthesis pathway (Fig. 1e). However, the maize kernel model was able to biosynthesize both pigments (Fig. 1e), indicating that iOSA3474-G successfully captured biologically meaningful phenotype of rice grain.

Connecting warmer night temperature (WNT) with grain chalkiness

As iOSA3474-G was able to predict biologically relevant phenotypes for the rice grain, we used this model to gain further insights on rice grain metabolism under WNT. For that, we used a published transcriptomic dataset for Dawn control/WNT, Dawn 7 h control/WNT, and Dusk control/WNT[22]. We selected only Dawn, Dawn 7 h, and Dusk from the entire transcriptome dataset to incorporate into our model because these three time points represent distinct phases within the circadian cycle. For instance, Desai et al.[22] referred to the 'Dawn' transcriptome when samples were collected at 6:15 AM, the first point of collection after higher nighttime respiration in WNT samples. The second time point of 1.15 PM will reflect the difference in energy status between control and WNT samples and the extent to which photosynthetic pathways are altered due to the previous warmer night. Finally, the dusk sample is a comparison between control and WNT grains before the initiation of the heat stress for the WNT samples. These three samples were used to represent the putative physiological

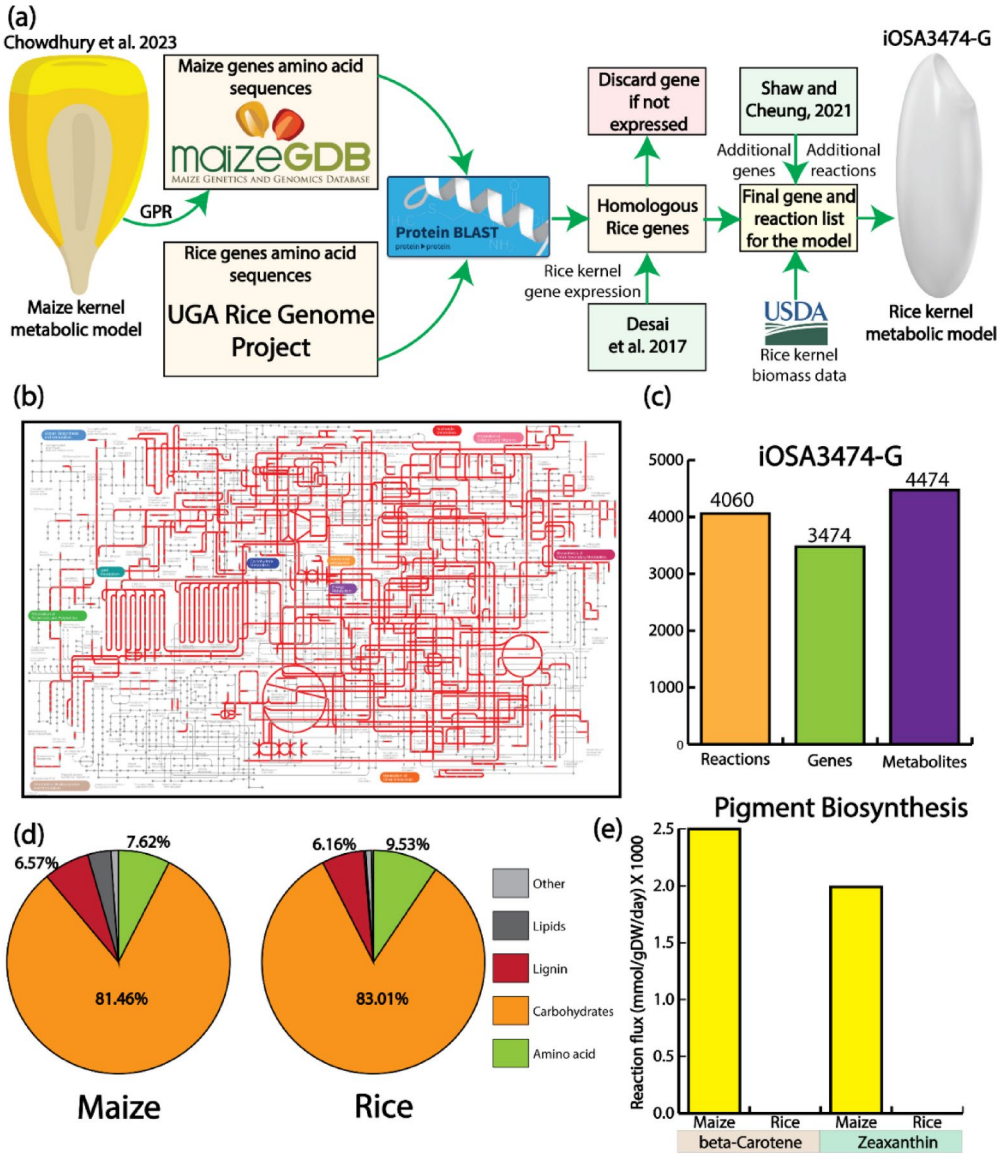

Fig. 1. Genome-scale metabolic model reconstruction of rice grain. (**a**) iOSA343474-G reconstruction through homology search against maize kernel metabolic model, literature search, and existing whole plant rice metabolic model. Biomass equation was reconstructed from the data obtained from USDA. (**b**) A metabolic network of iOSA3474-G generated from KEGG. (**c**) Statistic of the iOSA3474-G. (**d**) Biomass constituent comparison between maize kernel and rice grain. (**e**) iOSA3474-G cannot produce major pigments, beta-carotene and zeaxanthin, which maize kernel can produce.

status of the grains just before the initiation of warmer nighttime temperature, towards the end of the nighttime heating and mid-day status during peak carbon capture. Next, these transcriptomic data showed high degree of Pearson correlation (Fig. 2a). The lowest degree of correlation was found between Dawn control-Dawn 7 h control, Dawn WNT-Dawn 7 h WNT conditions, which was 0.79. This indicated 7 h after dawn, a transcriptomic response changes compared to the dawn conditions. This finding, in light of the overall transcriptome of the rice grain, reconfirms the findings from the previous study[22].

To project these transcriptomics data into the fluxomics space, we incorporated these transcriptomics data with iOSA3474-G using our recently developed tool called EXTREAM[18] (Fig. 2b). Rice panicle transcriptomics data is particularly well-suited to understanding rice grain metabolism, as the panicle itself contains the developing grains and serves as the central conduit for nutrient transfer and metabolic regulation throughout grain maturation. Key metabolic activities within the panicle—such as starch synthesis, lipid metabolism, and amino acid production—are crucial for grain development, providing essential precursors and controlling the energy dynamics necessary for grain filling. While grain chalkiness is often associated with later stages of development, transient heat stress during the first 1–4 days after fertilization can induce chalkiness at maturity[31,32]. Given that a panicle completes fertilization in 3–5 days, transcriptomic changes during this early period likely influence chalkiness. Our analysis (Supplementary Fig. S1) shows that warmer nights mis-

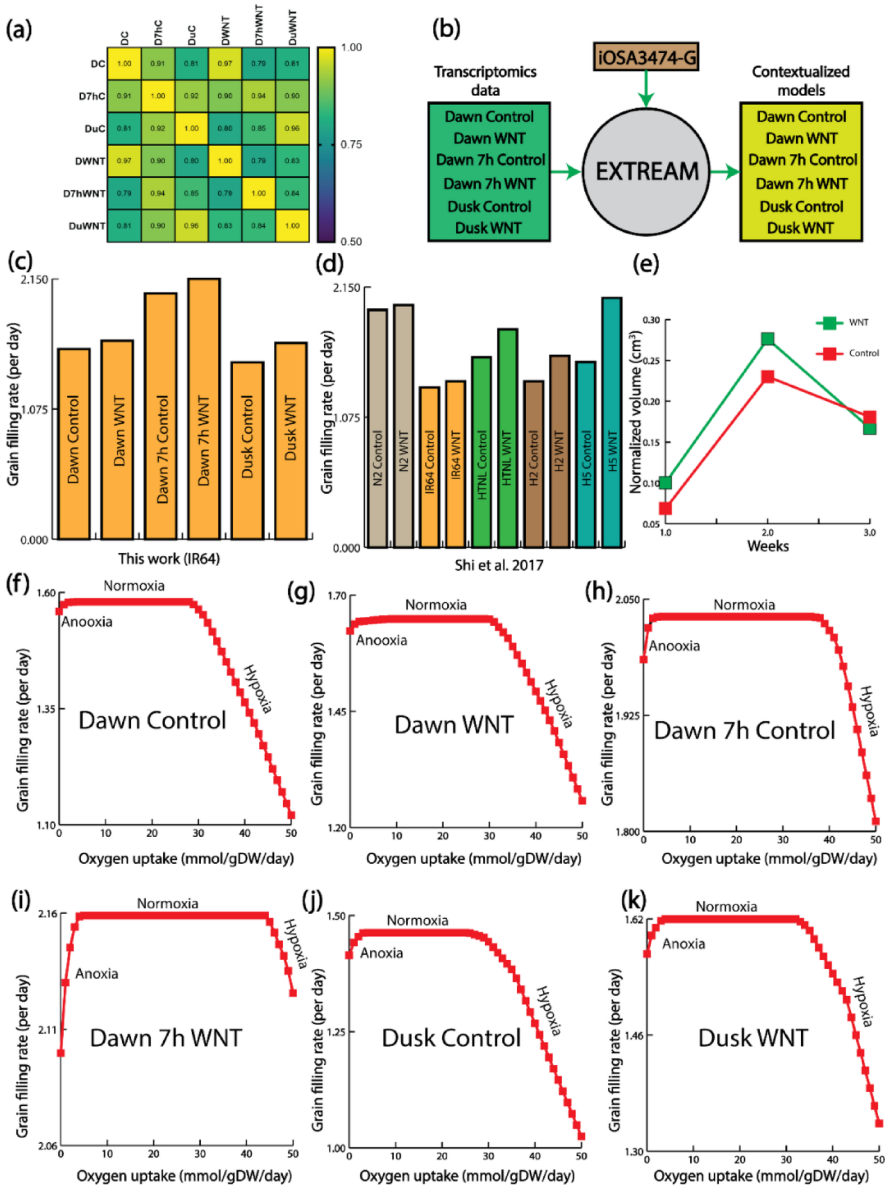

Fig. 2. Characterization of rice grain under warmer night temperature. (**a**) Dawn control/Dawn WNT, Dawn 7 h control/Dawn 7 h WNT, and Dusk control/Dusk WNT are strongly correlated, indicating a similar transcriptomic response between control and WNT conditions. (**b**) EXTREAM was used to reconstruct six contextualized models using transcriptomics data and iOSA3474-G. (**c**) Contextualized iOSA3474 predicted grain filling rates. (**d**) Grain filling rates from literature for different rice genotypes. (**e**) Experimentally measured grain volume data confirmed higher grain filling rate in WNT than control condition. (**f**) Grain filling rate with varying oxygen uptake for Dawn control. (**g**) Grain filling rate with varying oxygen uptake for Dawn WNT. (**h**) Grain filling rate with varying oxygen uptake for Dawn 7 h control. (**i**) Grain filling rate with varying oxygen uptake for Dawn 7 h WNT. (**j**) Grain filling rate with varying oxygen uptake for Dusk control. (**k**) Grain filling rate with varying oxygen uptake for Dusk WNT.

regulate genes associated with grain chalkiness[33–35], providing critical insights into how environmental stress impacts grain quality and yield, even in the earliest stages of development. EXTREAM previously predicted correct phenotypes for whole maize plant under control and temperature stress conditions and uncovered the role of energy production and reducing power generation in explaining metabolic bottlenecks of temperature stress conditions[18]. EXTREAM returned six contextualized models which were further probed to understand metabolic underpinnings of WNT conditions. Contextualized models predicted higher grain filling rates for WNT conditions (Fig. 2c). Previous studies[36] also predicted this pattern, not only for IR64, but also for other rice genotypes (Fig. 2d). *De novo* experimental data, calculating grain volume for control and WNT conditions, also supported the higher grain filling rate in the WNT conditions (Fig. 2e). Grain weight is determined by a balance between grain-filling rate and duration of grain filling. Although WNT conditions consistently showed higher grain filling rates, it was reported that, due to lack of assimilates[37] and loss of sink activity[38], an early

termination of grain filling in rice can occur under higher temperature. Moreover, photosynthesis, transpiration, and respiration are temperature-sensitive processes that contribute to grain weight. However, only respiration occurs consistently during the day and night. An increase in nighttime respiration has been associated with high nighttime temperatures. Therefore, increase in dark respiration is often considered as the primary mechanism for the observed high grain filling rate and decreased grain-filling duration[22].

In WNT, due to the reduced dark respiration, less oxygen is available for the grain[39]. Since the relationship among WNT, oxygen availability, and rice grain chalkiness has not been previously explored, we investigated whether grain growth changes with varying oxygen uptake. We plotted grain growth profile under all six different conditions and identified three different growth regions: anoxia (oxygen deficient), normoxia (normal oxygen), and hyperoxia (excess oxygen) (Fig. 2e–f), representing the lowest to highest possible oxygen intake across all conditions. A similar growth pattern was observed for the barley seed[40], although the normoxia phase in barley seed was brief. To our knowledge, this is the first study, reporting three distinct oxygen-dependent growth phases of grain development. Prior studies have shown that WNT induces chalkiness in rice grain[36] (Supplementary Fig. S2). We hypothesized that reduced oxygen availability during WNT conditions may cause chalkiness to emerge early in the normoxia phase, particularly because the oxygen demand in later part of normoxia may exceed what is realistically available in the atmosphere. Therefore, we focused our analysis on early normoxia, as it likely reflects the most physiologically relevant window for investigating the metabolic basis of grain chalkiness under WNT.

Histidine as the potential metabolic marker of normoxia and grain chalkiness

As it is hypothesized that chalkiness is more relevant in the early stage of normoxia, further characterization of early normoxia is required to understand relationship between oxygen availability and chalkiness. As all the three growth phases are readily visible in the Dawn 7 h WNT conditions (Fig. 2i), initial analysis for normoxia was conducted based on that condition. Some plants accelerate glycolysis under anoxia, a mechanism known as the 'Pasteur effect'[41]. This helps to alleviate the large reduction of energy produced by fermentation as compared with oxidative phosphorylation, especially during the early period of acclimation to anoxia[42]. Thus, under anoxia, grain should perform more substrate level phosphorylation compared to when more oxygen is available. iOSA3474-G interestingly predicted higher substrate level phosphorylation under early normoxia (Fig. 3a). As energy generation is restricted in the early normoxia, which is evident from, Fig. 3a (substrate-level phosphorylation) and Fig. 3d (restricted flux through succinate to fumarate), it is likely that subsequent catabolism of different pathways will also be restricted. That will be more applicable to lipid biosynthesis as rice grain has 0.24% lipid, contrary to the 3.4% lipid in maize kernel (Fig. 1d). Interestingly, similar to the substrate level phosphorylation, iOSA3474-G correctly predicted lower glycerolipid biosynthesis in early normoxia (Fig. 3b).

Grains serve as a sink tissue, which receive amino acids from the other part of the plant such as root, shoot, and leaf[43]. Therefore, we aimed to characterize the amino acids that are going to the grain through phloem. Compared to the other amino acids, during normoxia, we noticed very high glutamate uptake by the grain (Fig. 3c). As one of the major forms of nitrogen in rice[44], glutamate may have other functions in producing other amino acids (glutamate), TCA components (α-ketoglutarate), and nucleotides (AMP, purines, and pyrimidines), along with the activation of the chaperone function (mediated by HSP response) and antioxidant defence[45]. However, how high glutamate uptake through phloem is converted to biomass through other amino acids is still an unanswered question. Therefore, we used iOSA3474-G to check what is the conversion route of the accumulating glutamate to other amino acid that contributed to the biomass growth.

We tracked the high uptake of glutamate in the metabolic network and found the transport reaction which brings histidine from cytosol to biomass carried 4.38 time more flux in the early normoxia, (13.38 mmol/gDW/day of flux in the early normoxia, where as 3.06 mmol/gDW/day of flux towards in the late normoxia) (Fig. 3d). Next, through a sink reaction (Exchange_C00135[K, L]), histidine was sent to other parts of the plant, indicating the need of histidine transport from grain to other part of the tissue during WNT conditions (Supplementary Data S2). Thereby, this overproduction of histidine during the early normoxia can be considered a metabolic marker of chalkiness. Furthermore, tracking glutamate uptake revealed interesting pattern in the TCA cycle. In both early and late normoxia, glyoxylate shunt was turned off. Furthermore, TCA cycle was partially active and produced different metabolites through transport from other compartments (2-OG, glutamate, succinyl-CoA) or by catabolizing higher carbon sources (malonyl-CoA). Besides, it exports metabolites to cytosol as well (malate and citrate). Eventually, the citrate converts to histidine that aids in biomass production and supplying additional histidine to other parts of the plant. Compared to the late normoxia, early normoxia contributes 4.38 times more histidine to the biomass and other parts of the plant (Fig. 2d). Thus, histidine can be a metabolic marker to indicate chalkiness in the rice grain. Previous studies suggested higher histidine level in the less oxygenated condition, supporting the finding of this work[46]. For other WNT conditions, histidine also showed a similar contribution to the biomass and served as the metabolic marker. Interestingly, for the control conditions models, such a high contribution of Histidine was not noticed (Supplementary Data S2). The flux distribution for early and later stages of normoxia is now provided in Supplementary Data S2.

Tyrosine as the potential metabolic marker of hyperoxia and the evolutionary role of MDAR

We next analyzed the hyperoxic phase, characterized by availability of excess oxygen for the grain. Hyperoxic growth region is not a theoretical prediction, as it has been shown in the lab setting for maize kernel that higher partial pressure of oxygen reduced the overall kernel size[47]. From a previous study[47], hyperoxia had a modest impact on the number of responsive maize kernel genes, but caused a more rapid rate of kernel development. The most prominently downregulated gene under hyperoxia was a BAX inhibitor-1[48]. In Arabidopsis, this gene suppresses programed cell death. The downregulation of this inhibitor in maize kernels could thus lead

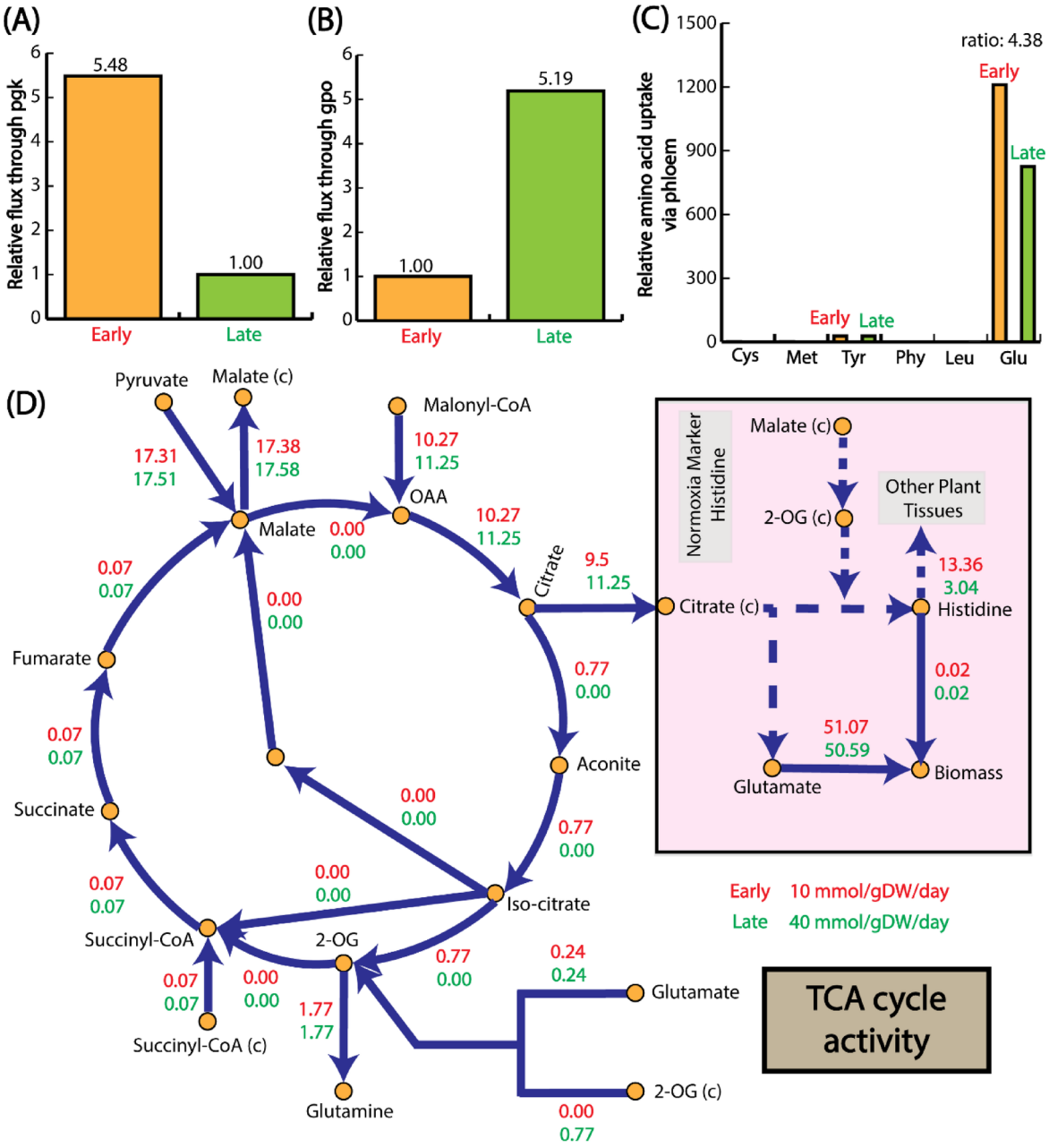

Fig. 3. Metabolic characteristic of normoxia. (**a**) Reduced substrate level phosphorylation. (**b**) Increased glycerolipid metabolism. (**c**) High phloem uptake of glutamate by the grain. (**d**) Metabolic network elucidating the role of histidine as a metabolic marker in grain chalkiness.

to an earlier onset of programed cell death, a characteristic feature of maturing endosperm. Another marker of more rapid kernel development under hyperoxia was the upregulation of an α-zein 3 storage protein typically expressed during late stages of maturation[49].

In the late hyperoxic growth phase, unlike glutamate in normoxia, grain uptakes 6.67 times higher amount of phenylalanine through phloem tissues compared to the early phase of hyperoxic growth phase (Fig. 4a). We tracked this high uptake of phenylalanine in the metabolic network and found that the transport reaction which brings tyrosine from cytosol to biomass carries much higher flux in the late hyperoxia compared to the early hyperoxia (Fig. 4b). Similar to the histidine, this overproduction tyrosine also contributed to the other parts of the plant through a sink reaction, Exchange_C00082[K, L] (Supplementary Data S2). Previous study also supported elevated amount of tyrosine under comparatively high oxygen level[46]. Just like histidine in the normoxia, for the control conditions models, such a high contribution of tyrosine was not noticed (Supplementary Data S2). The flux distribution for early and later stages of hyperoxia is now provided in the Supplementary Data S2.

We also wanted to check where the excess oxygen is being used in the metabolic network in the hyperoxic phase of growth, to understand the grain's ability to use oxygen. We observed glycerol-3- phosphate being used

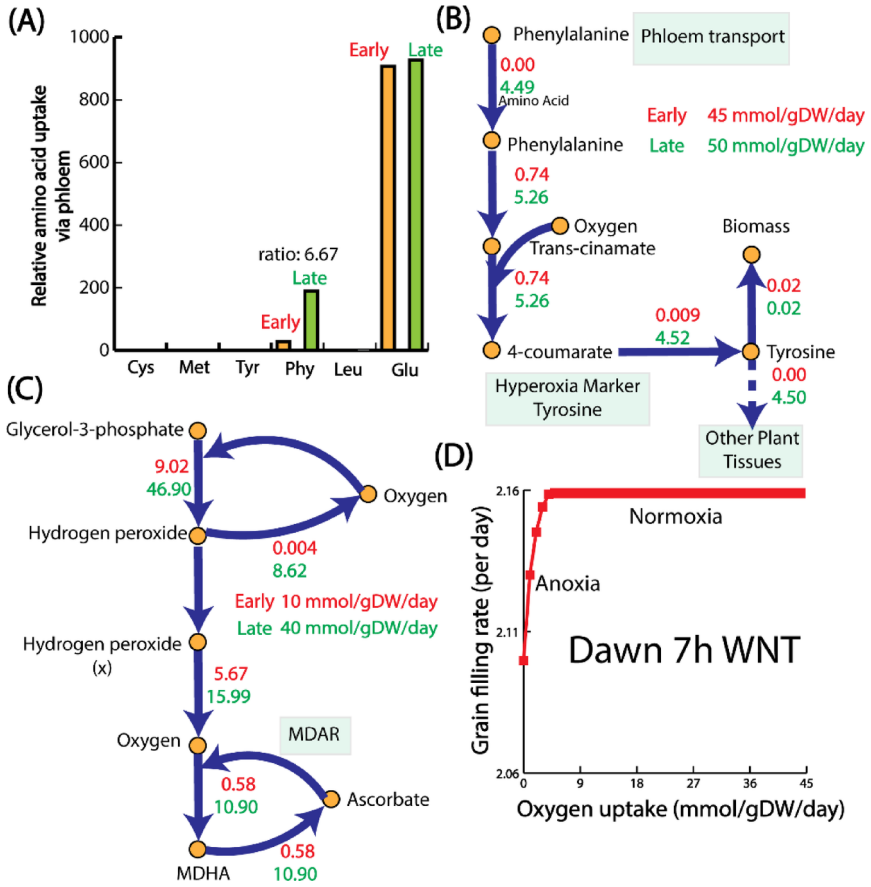

Fig. 4. Metabolic characteristic of hyperoxia and the evolutionary role of MDAR. (**a**) High phloem uptake of phenylalanine by the grain. (**b**) Metabolic network elucidating the role of tyrosine as a metabolic marker in hyperoxia. (**c**) Excess oxygen is being processed by monodehydroascorbate reductase (MDAR). (**d**) If MDAR is knocked out, hyperoxic phase no longer exist.

to produce hydrogen peroxide, which recycled back to oxygen to produce monodehydroascorbate (MDAR). The MDAR recycled back to oxygen with an ascorbate intermediate (Fig. 4c). This step is catalyzed by an enzyme, monodehydroascorbate reductase (MDAR). MDAR plays a key role in stress tolerance and ascorbate metabolism in plants. MDAR activities have been reported in algae[50], bryophytes[51] and higher order plants[52]. Moreover, MDAR is one of the key anti-oxidant enzymes responsible for scavenging reactive oxygen species[53] and supports the use of excess oxygen by grain through MDAR. When we turn off the MDAR reaction in iOSA3474-G, the hyperoxic phase no longer existed (Fig. 4d), indicating an essential role of MDAR in scavenging excess oxygen. From an evolutionary perspective, during the carboniferous era (300 to 35 million years ago), atmospheric oxygen levels was 35%[54]. Spermatophytes encompass the angiosperms and the gymnosperms, whose seeds are not enclosed in an ovary. The two groups diverged around 300 million years ago during the carboniferous era[55]. Thus, to survive the excess oxygen of carboniferous era, plant evolved the metabolic pathways involving MDAR. However, currently, with much lower current oxygen content in the atmosphere (21%), it is plausible that the MDAR activity in the rice grain is a remnant trait from the carboniferous era.

Potential role of nucleotide diphosphate kinase and Enoyl-CoA hydratase in WNT

With a comprehensive understanding of the various growth stages of rice grains in the WNT, next we implemented Metabolic Bottleneck Analysis (MBA)[18] on six different contextualized models to see how the metabolic bottlenecks changed dynamically in WNT conditions and impacted grain chalkiness. The MBA algorithm expands the flux space of each reaction in a GSM and assess its impact on the biomass growth rate, thereby returns bottleneck reactions. However, we now extended the MBA to return tentative bottleneck genes as well, using the gene-protein-reaction (GPR) association of bottleneck reactions (Fig. 5a). In this work, we identified 416, 409, 411, 432, 290, and 443 tentative bottleneck genes in Dawn control, Dawn WNT, Dawn 7 h control, Dawn 7 h WNT, Dusk control¸ and Dusk WNT, respectively (Supplementary Fig. S3). Details of all the genes can be found in the Supplementary Data S3. We also performed gene ontology analysis of control and WNT conditions. For all the control conditions, bottleneck genes were pertinent to cellular response to oxidative stress, response to oxygen-containing compounds, phosphorylation, organonitrogen compound metabolic process, etc. (Supplementary Fig. S4). This indicated that, all the control conditions have similar kind

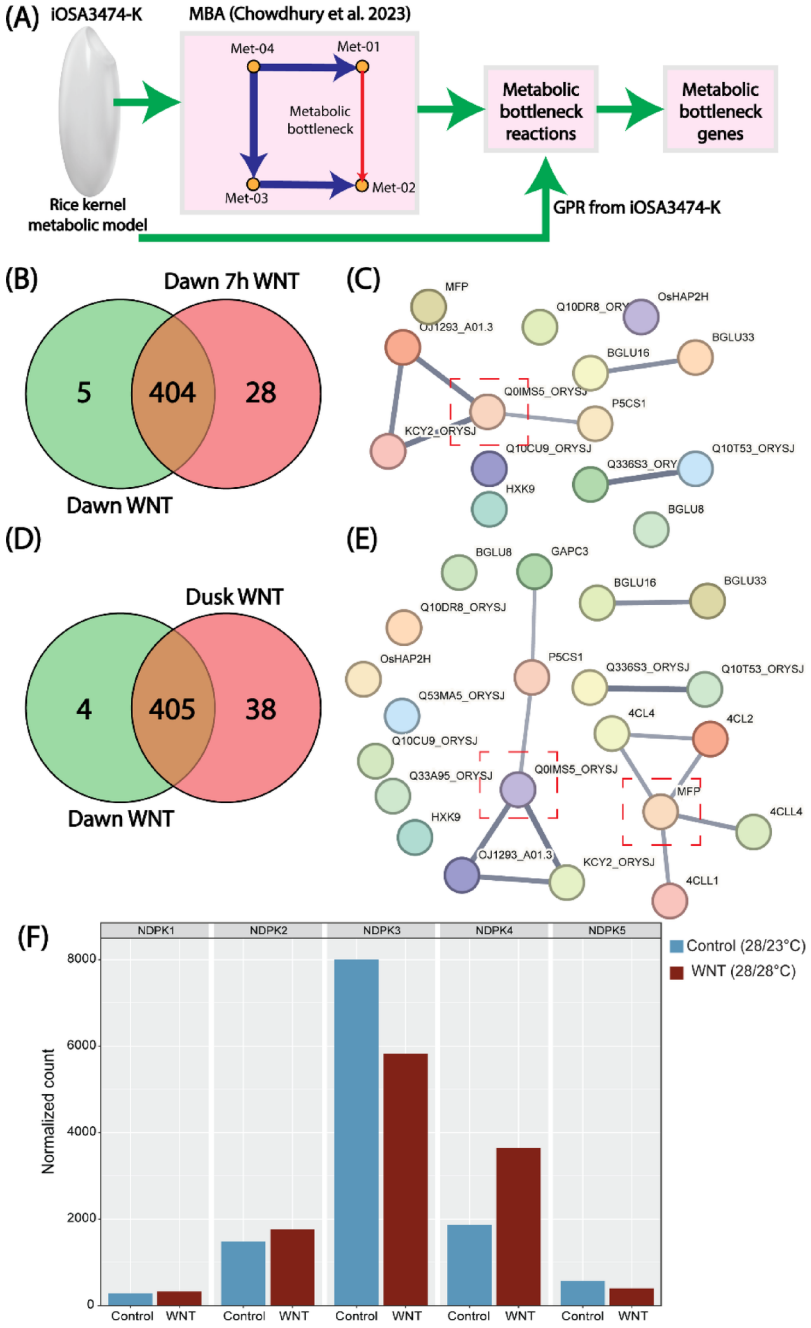

Fig. 5. Metabolic Bottlenecks Analysis (MBA) revealed the role of Nucleotide Diphosphate Kinase and Enoyl-CoA Hydratase in WNT. (**a**) Framework to find metabolic bottleneck genes using MBA and GPR. (**b**) Venn diagram showing unique and overlapped genes between Dawn WNT and Dawn 7 h WNT. (**c**) Protein-protein interaction network of 28 unique bottleneck genes of Dawn 7 h WNT indicates the regulatory role of nucleotide diphosphate kinase (Q0IMS5_ORYSJ) (red box). (**d**) Venn diagram showing unique and overlapped genes between Dawn WNT and Dusk WNT. (**e**) Protein-protein interaction network of 38 unique bottleneck genes of Dusk WNT indicates the regulatory role of nucleotide diphosphate kinase (Q0IMS5_ORYSJ) and enoyl-CoA hydratase (MFP) (red boxes). (**f**) expression analysis of five different nucleotide diphosphate kinase genes.

of bottlenecks and behaved similarly. Correlation of transcriptomics data (Fig. 2a) for all the control conditions also supports this (lowest correlation 0.81, between Dawn control and Dusk control conditions).

Interestingly, gene ontology analysis revealed different functionality of bottleneck genes in different WNT conditions (Supplementary Fig. S5). In Dawn WNT condition, bottleneck genes are mostly from phosphorylation, small molecule metabolic process, and phosphate-containing compound metabolic process. Interestingly, in the Dawn 7 h WNT condition, bottleneck genes are associated with cellular responses to oxidative processes, reactive oxygen species metabolic processes, and phosphorylation, among others. Conversely, for the Dusk

WNT condition, bottleneck genes are linked to purine-containing compound metabolic processes, nucleobase-containing small molecule metabolic processes, and phosphorylation. Notably, phosphorylation emerges as a consistent top bottleneck process across all three WNT conditions, as revealed by gene ontology analysis. A previous study revealed that phosphorylation might play specific roles in amylopectin biosynthesis only in response to high-temperature stress for rice grain through different phosphorylation motifs such as sP, LxRxxs, and tP[56]. As WNT conditions are metabolically distinct from each other, we next analyzed how metabolic bottlenecks dynamically progressed along the day compared to the Dawn WNT conditions.

Between Dawn WNT and Dawn 7 h WNT conditions, there were 5 bottleneck genes that were unique to the Dawn WNT condition (Fig. 5b). These are transcription initiation factor TFIID subunit 10, glutamine amidotransferase, cytidylyltransferase, pentatricopeptide, and urease. A gene ontology analysis revealed these genes are associated with nickel insertion and nickel cation binding. Nickel cation is a cofactor for certain enzymes, including urease, which is involved in nitrogen metabolism. A previous study[57] showed that nitrogen metabolism played spatial and temporal regulations in tissue (or stress)-specific way, indicating the importance of nitrogen metabolism in growth, development and stress responses. For the Dawn 7 h WNT condition, there were 28 bottleneck genes that were unique to the Dawn 7 h WNT condition (Fig. 5b). A protein-protein interaction network revealed the central role of nucleotide diphosphate kinase in regulating bottleneck genes in Dawn 7 h WNT (Fig. 5c). Interestingly, nucleoside diphosphate kinase converts GTP to GDP, which is a key reaction in the ppGpp biosynthesis pathway. ppGpp is a stress regulator in many plants and bacteria[58]. Between Dawn WNT and Dusk WNT conditions, there were 4 bottleneck genes that were unique to the Dawn WNT condition (Fig. 5d). Apart from cytidylyltransferase, all other genes were similar to the unique Dawn WNT condition of Dawn WNT vs. Dawn 7 h WNT conditions, impacting nitrogen metabolism. For the Dusk WNT condition, there were 38 bottleneck genes that were unique to the Dusk WNT condition (Fig. 5d). A protein-protein interaction network revealed the central role of nucleotide diphosphate kinase (NDPK), like the Dawn WNT vs. Dawn 7 h WNT conditions (Fig. 5e). The rice genome contains five NDPKs. To determine the possible NDPK that may be responsive to WNT conditions in rice, we examined the expression of these five genes in rice grain transcriptome dataset for control and WNT stress[59]. Two of these genes, *OsNDPK3* and *OsNDPK4* were expressed strongly in rice grains relative to other gene family members (Fig. 5f). Expression of *OsNDPK4* is induced by the WNT stress, while transcript abundance of *NDPK3* decreased under WNT stress. Since NDPKs have a central role in energy utilization, a change in transcript abundance leading to differential enzymatic activity, could alter the ratio of carbon directed towards starch biosynthesis via ADP-glucose versus cell wall via UDP-glucose[60]. Additionally, enoyl-CoA hydratase was also involved in regulating bottleneck genes in Dusk WNT. Enoyl-CoA hydratase is an important step in the β-oxidation, and interestingly it was shown for wheat that, up-regulation of genes belonging to fatty acid β-oxidation pathway[61].

To understand the temporal WNT responsiveness of the bottleneck genes, we analyzed the expression of all 451 genes in the published transcriptome dataset generated from developing rice panicles treated with WNT stress along with the controls[22]. Our clustering analysis revealed that expression of 67 genes was relatively high under WNT (Dawn 7 h) compared to control conditions (Fig. 6a). GO analysis of the cluster showed the enrichment of ATP related terms such as 'ATP binding', 'ATP hydrolysis activity', 'ATPase complex' and 'ATPase-coupled transmembrane transporter activity' (Supplementary Fig. S6). Among these genes, we found six subunits of ATP synthase and four ATP binding ABC transporters. Besides these genes, the cluster also consists of five vacuolar ATP synthases.

ATP synthase complex, in particular vacuolar ATPase is known to play a role in response to oxidative stress, which indicates the WNT response role of genes in the cluster as the high temperature triggers cellular oxidative stress[62]. For instance, the previous genetic study showed that an overaccumulation mutation in subunit E isoform 1 of the vacuolar H+-ATPase (*LOC_Os01g46980*) led to floury grain phenotype[63], wherein a similar developmental defect has also been observed in grain developed under WNT conditions[64]. In addition to the genes induced by stress, 53 genes are found to be suppressed by WNT during the daytime (Dawn 17.5 h) (Fig. 6b). This cluster is primarily enriched in genes with a function such as 'catalytic activity', 'ion binding' and 'small molecule binding'. Arabidopsis ortholog of two aldehyde oxidase coding genes (*LOC_Os03g57690* and *LOC_Os03g57680*) in the cluster catalyzes the abscisic acid (ABA) biosynthesis. Suppression of these ABA-related genes, a regulator of seed development and maturation, indicates that an imbalance in ABA concentration under WNT contributes to the distortion of seed development.

In summary, this study introduces the first-ever rice grain genome-scale metabolic model (GSM), iOSA3474-G, and investigates the impact of warmer night temperatures (WNT) on rice kernel quality, particularly chalkiness, due to global warming. Through computational approach, this work predicted metabolic markers like histidine and tyrosine linked to different growth phases under WNT conditions. Importantly, we have predicted MDAR and nucleoside diphosphate kinase as regulators of metabolic flux. These findings present new perspectives into understanding grain chalkiness in rice and lay the groundwork for innovative approaches to bolster crop resilience in the face of environmental challenges.

Materials and methods

iOSA3474-G reconstruction

We used the maize kernel model from iZMA6517[18] as the template to reconstruct the iOSA3474-G. Although maize genome has more than 20,000 genes, the maize kernel model only consisted of genes which takes part in the metabolism only. We downloaded the amino acid sequence for all the maize kernel genes from the MaizeGDB website. We collected amino acid sequence of all the genes for the entire IR-64 rice genome from the UGA Rice Genome Project[65]. We then performed bi-directional blast between maize kernel genes from iZMA6517 and entire rice genome. Out of 6257 genes from the maize kernel, 3269 genes was matched with rice grain with an E-score 0.0, resembling high degree of homology between maize kernel and rice grain. The highest

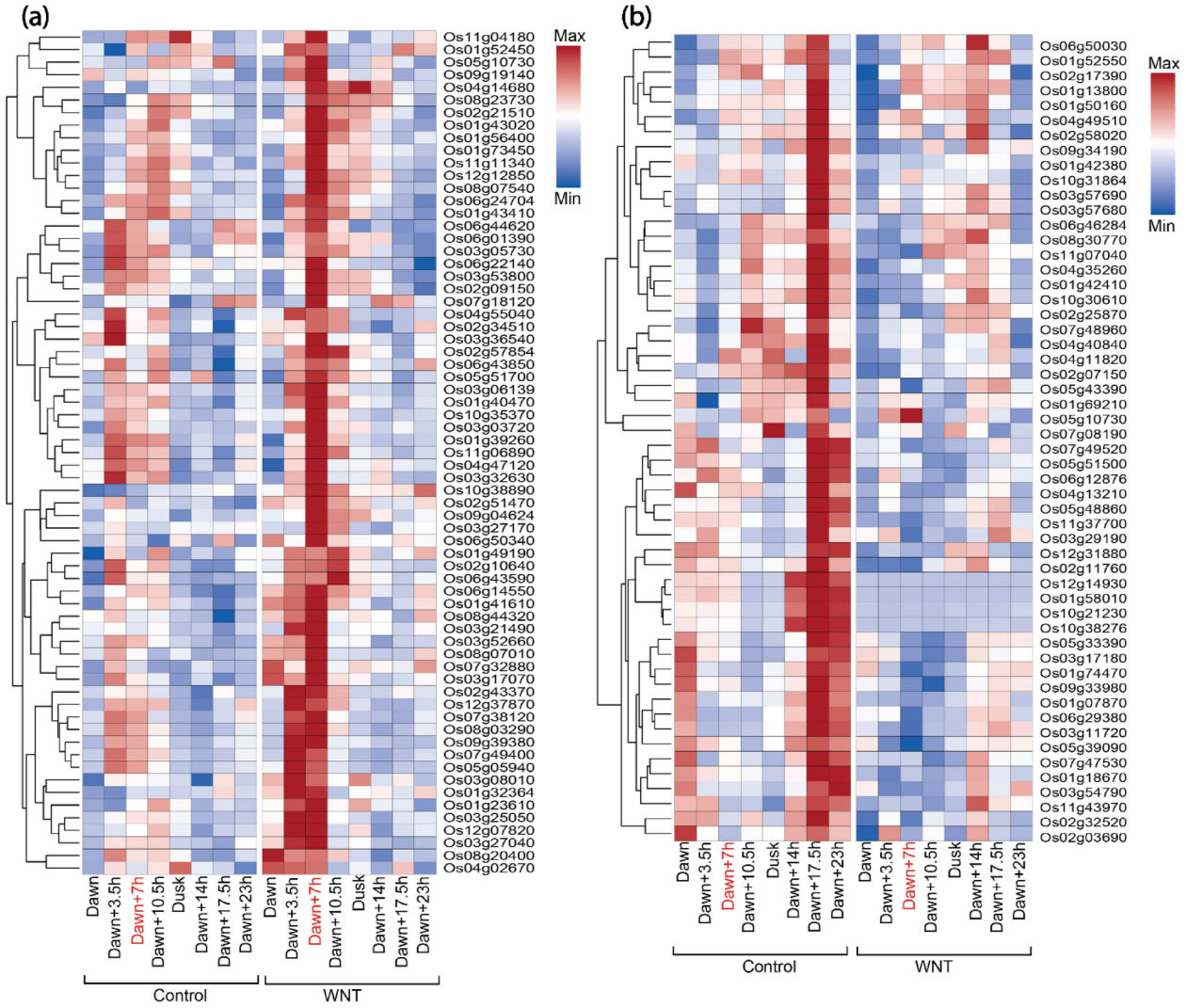

Fig. 6. Two clusters derived from bottleneck genes showed highly similar responses to the temporal WNT treatment study. (**a**) K-means clustering analysis showed that expression patterns of 67 genes are induced under WNT at Dawn + 7 compared to the control conditions. (**b**) Expression of 53 genes in suppressed in response to WNT at Dawn + 17.5 h.

E-value for rice grain gene recorded was 9.5E-06 for *LOC_Os04g56710* and *LOC_Os02g11760* (Supplementary Data S4). Eventually, all the maize kernel genes from iZMA6517 has homologue in rice kernel. Moreover, the blast identified same rice grain genes for multiple maize kernel genes, thereby we automatically removed those duplicates rice grain genes from the model through an automatic python scripting. GPR for all the reactions were manually curated from the KEGG and Rice Genome Project database. For all biomass precursors, we included transport reactions from the cytosol to the biomass compartment, enabling us to quantify each precursor's contribution to biomass synthesis. Moreover, as with changing conditions sink tissue can also works as a source tissue[66], we have added sink reactions to the model for important metabolites (Supplementary Data S2). As a result, 2899 out of 4060 reactions (71%) has GPR relationship. In addition, We collected expression data from literature (Desai et al., 2021)to see how many of those rice genes were expressed. If not expressed, those genes were discarded from the model. Next, we took a previously published rice grain model (Shaw and Cheung, 2021a) and collected genes and reactions which were not part of the newly reconstructed draft model. For the genes, only those were added to the draft model which had expression values found in literature (Desai et al., 2021). From the multi-organ metabolic model of rice (Shaw and Cheung, 2021b), we only considered those reactions which were not part of the draft model. Overall, since the model is based on iZMA6517, which is fully mass balanced, thereby further description on the model's mass balanced is not discussed in this work. Subsequently, we determined compartments for those reactions using CELLO (Yu et al., 2006), and added to the draft model. GAMS, in conjunction with the CPLEX solver, was employed to tackle all optimization challenges. The NEOS server offers an alternative for executing GAMS codes without necessitating a license purchase. A comprehensive guide for running GAMS codes on the NEOS server is available in the literature (Chowdhury et

al., 2022a). Additionally, to cater to the convenience of COBRApy users, an SBML version of the iOSA3474-G is provided.

Expression distributed reaction flux measurement (EXTREAM)

The formulation of EXTREAM is the following:

$$min \sum_{j} (|v_j| - v_{j,\ omics})$$

Subject to,

$$\sum_{j} S_{i,j} v_j = 0, \forall i \in I \tag{1}$$

$$v_{j,min} \leq v_j \leq v_{j,max}, \forall j \in J \tag{2}$$

$$v_{biomass} \leq f \times v_{biomass,max} \tag{3}$$

Here, v_j is the flux to be calculated for reaction J, $v_{j,omics}$ is the reference condition calculated from the gene-protein-reaction association for reaction J, $S_{i,j}$ is the stoichiometric matrix for metabolite I, and reaction J, $v_{j,min}$ and $v_{j,max}$ are the upper and lower bound of reaction J, $v_{biomass}$ is the desired biomass growth rate, $v_{biomass,\ max}$ is the maximum possible biomass growth rate, and f is fraction between 0 and 1. To reformulation of EXTREAM algorithm to a linear optimization problem can be found in our previous work (Chowdhury et al., 2023). Predicted flux solution for each of the contextualized model is provided in Supplementary Data S2.

Parsimonious flux balance analysis (pFBA)

pFBA (Lewis et al., 2010) is constrained based optimization technique to model GSMs. The pseudo-steady state mass balance in pFBA is represented by a stoichiometric matrix, where the columns represent metabolites, and the rows represent reactions. For each reaction, upper and lower bounds is imposed based on thermodynamic information. pFBA provides the flux value for each reaction in the model according by solving the following optimization problem:

$$\max \quad v_{biomass} - 0.0001 \sum_{j \in J} |v_j|$$

$$Subject\ to:$$

$$\sum_{j \in J} S_{ij} v_j = 0, \forall i \in I \tag{4}$$

$$a_j \leq v_j \leq b_j \tag{5}$$

In this formulation, I is the set of metabolites and J is the set of reactions in the model. S_{ij} is the stoichiometric matrix with i indicating metabolites and j indicating reactions, and v_j is the flux value of each reaction. The objective function, $v_{biomass}$, is the proxy of the growth rate of an individual cell. a_j and b_j are the lower and upper bounds of flux values for each reaction. For forward reactions, the highest possible bounds were 0 mmol/gDW/h to 1000 mmol/gDW/h. For the reversible reactions, the highest possible bounds were $-1000\frac{mmol}{gDW.day}$ to $1000\frac{mmol}{gDW.day}$.

Metabolic bottleneck analysis

To determine the metabolic bottleneck in a GSM metabolic bottleneck analysis (Chowdhury et al., 2023)was used. The formulation is as following.

$$\left[\begin{array}{ll} Max\ v_{biomass} & \\ Subject\ to: & \\ \sum_{j=1}^{m} S_{ij} v_j = 0, i \in I & (6) \\ a_j \leq v_j \leq b_j, j/\{j'\} \in J & (7) \\ v_{j',\min,} \leq v_{j'} \leq v_{j',\max}, j' \in J & (8) \end{array}\right], \forall j' \in J$$

Here a_j is the lower bound reaction v_j and b_j is the upper bound of reaction v_j. Both a_j and b_j were calculated from the transcriptomics data and gene-protein-reaction association. $v_{j',\ min}$ is the expanded lower bound of the reaction j' and $v_{j',\ max}$ is the expanded upper bound of the reaction j'. In this case, we set $v_{j',\ min} = -1000\frac{mmol}{gDW.day}$ and $v_{j',\ max} = 1000\frac{mmol}{gDW.day}$. We solved the optimization problem by maximizing the biomass $v_{biomass}$ for the new expanded flux space of each reaction j' in an iterative manner and then recorded the biomass growth rate. From this biomass growth rate collections, we can check for which j' biomass growth rate increased significantly. Then that j' can be considered as the metabolic bottleneck of a given metabolic network.

Grain volume measurement for control and WNT conditions

We used the PI-PLAT imaging system to capture RGB digital images of primary panicles for 3D reconstruction, following the method described by Sandhu et al. (2019). For each panicle from control and WNT-treated plants, a total of 120 images were captured at 360° coverage using two Sony α6500 digital cameras. Illumination was provided by an LED light source (ESDDI PLV-380, 15 W, 5000 LM, 5600 K), and the cameras were mounted on a rotating wheel driven by an electric motor system to ensure consistent speed and coverage. During image processing, the captured RGB images were converted into hue-saturation-value (HSV) space, and background elements such as the imaging chamber and wooden board were removed. A denoising step was applied to eliminate any remaining background artifacts. The pre-processed images were then used to generate a 3D point cloud of each panicle using the MVE pipeline. Point clouds were subsequently segmented and scaled to a uniform reference by utilizing the positional information of colors. Finally, volumetric quantification was performed by voxelizing the point clouds.

Software and hardware resources

The General Algebraic Modeling System (GAMS) version 24.7.4 with IBM CPLEX solver was used to run pFBA, EXTREAM, and MBA algorithm on the model. Each of the algorithm was scripted in GAMS and then run on a Linux-based high-performance cluster computing system at the University of Nebraska-Lincoln. The model is also available in the systems biology markup language.

Data availability

The data that support for the findings of this study can be found in the related cited articles and/or in the supplementary data. All the codes used to generate these results can be accessed in the GitHub repository (https://github.com/ssbio/-rice_grain).

Received: 25 January 2025; Accepted: 28 April 2025
Published online: 12 May 2025

References

1. Yuan, S. et al. Sustainable intensification for a larger global rice bowl. *Nat. Commun.* **12**, 7163 (2021).
2. Roberts, L. 9 Billion? *Science* **333**, 540–543 (1979). (2011).
3. He, Y., Wu, Z., Liu, X. & Deng, F. Analysis of surface air temperature variations and local urbanization effects on central Yunnan plateau, SW China. *Theor. Appl. Climatol.* **131**, 101–110 (2018).
4. Lyman, N. B., Jagadish, K. S. V., Nalley, L. L., Dixon, B. L. & Siebenmorgen, T. Neglecting rice milling yield and quality underestimates economic losses from High-Temperature stress. *PLoS One*. **8**, e72157 (2013).
5. Sillmann, J., Donat, M. G., Fyfe, J. C. & Zwiers, F. W. Observed and simulated temperature extremes during the recent warming hiatus. *Environ. Res. Lett.* **9**, 64023 (2014).
6. Impa, S. M. et al. High night temperature effects on wheat and rice: Current status and way forward. *Plant Cell and Environment* vol. 44 Preprint at (2021). https://doi.org/10.1111/pce.14028
7. Mohammed, A. R. & Tarpley, L. Effects of high night temperature and spikelet position on yield-related parameters of rice (Oryza sativa L.) plants. *Eur. J. Agron.* **33**, 117–123 (2010).
8. Coast, O., Murdoch, A. J., Ellis, R. H., Hay, F. R. & Jagadish, K. S. V. Resilience of rice (Oryza spp.) pollen germination and tube growth to temperature stress. *Plant. Cell. Environ.* **39**, 26–37 (2016).
9. Cao, Z. et al. Comprehensive expression of various genes involved in storage protein synthesis in filling rice grain as affected by high temperature. *Plant. Growth Regul.* **81**, 477–488 (2017).
10. Nakamura, Y., Yuki, K., Park, S. Y. & Ohya, T. Carbohydrate metabolism in the developing endosperm of rice grains. *Plant. Cell. Physiol.* **30**, 833–839 (1989).
11. Bahuguna, R. N., Solis, C. A., Shi, W. & Jagadish, K. S. V. Post-flowering night respiration and altered sink activity account for high night temperature-induced grain yield and quality loss in rice (Oryza sativa L). *Physiol. Plant.* **159**, 59–73 (2017).
12. Lanning, S. B., Siebenmorgen, T. J., Counce, P. A., Ambardekar, A. A. & Mauromoustakos, A. Extreme nighttime air temperatures in 2010 impact rice chalkiness and milling quality. *Field Crops Res.* **124**, 132–136 (2011).
13. Ashida, K., Iida, S., Yasui, T. & Morphological Physical, and chemical properties of grain and flour from Chalky rice mutants. *Cereal Chem.* **86**, 225–231 (2009).
14. Zhao, X. & Fitzgerald, M. Climate change: implications for the yield of edible rice. *PLoS One*. **8**, e66218 (2013).
15. Alsiyabi, A., Chowdhury, N. B., Long, D. & Saha, R. Enhancing in Silico strain design predictions through next generation metabolic modeling approaches. *Biotechnol. Adv.* **54**, 107806 (2022).
16. Orth, J. et al. What is flux balance analysis? *Nat. Biotechnol.* **28**, 245–248 (2010).
17. Chowdhury, N. B. et al. Dissecting the metabolic reprogramming of maize root under nitrogen-deficient stress conditions. *J. Exp. Bot.* **73**, 275–291 (2022).
18. Chowdhury, N. B. et al. A multi-organ maize metabolic model connects temperature stress with energy production and reducing power generation. *iScience* 26, (2023).
19. Chatterjee, A., Huma, B., Shaw, R. & Kundu, S. Reconstruction of Oryza sativa indica genome scale metabolic model and its responses to varying RuBisCO activity, light intensity, and enzymatic cost conditions. *Front. Plant. Sci.* **8**, 1–18 (2017).
20. Lakshmanan, M. et al. Unraveling the light-specific metabolic and regulatory signatures of rice through combined in Silico modeling and multiomics analysis. *Plant. Physiol.* **169**, (2015).
21. Shaw, R. & Cheung, C. Y. M. Integration of crop growth model and constraint-based metabolic model predicts metabolic changes over rice plant development under water-limited stress. *Silico Plants*. **3**, diab020 (2021).
22. Desai, J. S. et al. Warm nights disrupt transcriptome rhythms in field-grown rice panicles. *Proceedings of the National Academy of Sciences* 118, e2025899118 (2021).
23. Kim, J. J. et al. Cytosolic monodehydroascorbate reductase gene affects stress adaptation and grain yield under paddy field conditions in Oryza sativa L. japonica. *Mol. Breeding* **37**, (2017).
24. Murat, F., Armero, A., Pont, C., Klopp, C. & Salse, J. Reconstructing the genome of the most recent common ancestor of flowering plants. *Nat. Genet.* **49**, 490–496 (2017).
25. Paterson, A. H. et al. Convergent domestication of cereal crops by independent mutations at corresponding genetic loci. *Sci. (1979)*. **269**, 1714–1718 (1995).
26. Li, Y. et al. Natural variation in GS5 plays an important role in regulating grain size and yield in rice. *Nat. Genet.* **43**, 1266–1269 (2011).

27. Dong, G., Xiong, H., Zeng, W., Li, J. & Du, D. Ectopic expression of the rice Grain-Size-Affecting gene GS5 in maize affects kernel size by regulating endosperm starch synthesis. *Genes (Basel)* **13**, (2022).
28. Chan, S. H. J., Cai, J., Wang, L., Simons-Senftle, M. N. & Maranas, C. D. Standardizing biomass reactions and ensuring complete mass balance in genome-scale metabolic models. *Bioinformatics* **33**, 3603–3609 (2017).
29. Zhao, D., Zhang, C., Li, Q. & Liu, Q. Genetic control of grain appearance quality in rice. *Biotechnol. Adv.* **60**, 108014 (2022).
30. Song, J. et al. Carotenoid composition and changes in sweet and field corn (Zea mays) during kernel development. *Cereal Chem.* **93**, 409–413 (2016).
31. Nalini Chandran, A. K. et al. Phenotypic and transcriptomic responses of diverse rice accessions to transient heat stress during early grain development. *Front. Plant. Sci.* **15**, 1429697 (2024).
32. Paul, P. et al. Divergent phenotypic response of rice accessions to transient heat stress during early seed development. *Plant. Direct* **4**, (2020).
33. Dong, N. et al. OsLESV and OsESV1 promote transitory and storage starch biosynthesis to determine rice grain quality and yield. *Plant. Commun.* **5**, 100893 (2024).
34. Pan, Y. et al. Natural variation in OsMKK3 contributes to grain size and chalkiness in rice. *Front. Plant. Sci.* **12**, (2021).
35. Li, Y. et al. Chalk5 encodes a vacuolar H + -translocating pyrophosphatase influencing grain chalkiness in rice. *Nat. Genet.* **46**, (2014).
36. Shi, W. et al. High day- and night-time temperatures affect grain growth dynamics in contrasting rice genotypes. *J. Exp. Bot.* **68**, 5233–5245 (2017).
37. Kobata, T. & Uemuki, N. High temperatures during the grain-Filling period do not reduce the potential grain dry matter increase of rice. *Agron. J.* **96**, 406–414 (2004).
38. Kim, J. et al. Relationship between grain filling duration and leaf senescence of temperate rice under high temperature. *Field Crops Res.* **122**, 207–213 (2011).
39. Posch, B. C. et al. Wheat respiratory O2 consumption falls with night warming alongside greater respiratory CO2loss and reduced biomass. *J. Exp. Bot.* **73**, (2022).
40. Grafahrend-Belau, E., Schreiber, F., Koschützki, D. & Junker, B. H. Flux balance analysis of barley seeds: A computational approach to study systemic properties of central metabolism. *Plant. Physiol.* **149**, 585–598 (2009).
41. Barker, J., Khan, M. A. A. & Solomos, T. Mechanism of the Pasteur effect. *Nature* **201**, (1964).
42. Greenway, H. & Gibbs, J. Mechanisms of anoxia tolerance in plants. II. Energy requirements for maintenance and energy distribution to essential processes. *Funct. Plant Biol.* **30**, 999–1036 (2003).
43. Egli, D. B. & Bruening, W. P. Source-sink relationships, seed sucrose levels and seed growth rates in soybean. *Ann. Bot.* **88**, 235–242 (2001).
44. Fukumorita, T., Chino, M. & Sugar Amino acid and inorganic contents in rice phloem Sap. *Plant. Cell. Physiol.* **23**, 273–283 (1982).
45. Cruzat, V. et al. R. Metabolism and Immune Function, Supplementation and Clinical Translation. *Nutrients* vol. 10 Preprint at (2018). https://doi.org/10.3390/nu10111564
46. Zhang, G. et al. Comparative multi-omics analysis of hypoxic germination tolerance in weedy rice embryos and coleoptiles. *Genomics* **113**, 3337–3348 (2021).
47. Langer, M. et al. Causes and consequences of endogenous hypoxia on growth and metabolism of developing maize kernels. *Plant. Physiol.* **192**, 1268–1288 (2023).
48. Watanabe, N. & Lam, E. Bax Inhibitor-1, a Conserved Cell Death Suppressor, Is a Key Molecular Switch Downstream from a Variety of Biotic and Abiotic Stress Signals in Plants. *International Journal of Molecular Sciences* vol. 10 3149–3167 Preprint at (2009). https://doi.org/10.3390/ijms10073149
49. Stelpflug, S. C. et al. An expanded maize gene expression atlas based on RNA sequencing and its use to explore root development. *Plant. Genome* **9**, (2016). plantgenome2015.04.0025.
50. Haghjou, M. M., Shariati, M. & Smirnoff, N. The effect of acute high light and low temperature stresses on the ascorbate–glutathione cycle and superoxide dismutase activity in two Dunaliella salina strains. *Physiol. Plant.* **135**, 272–280 (2009).
51. Lunde, C., Baumann, U., Shirley, N. J., Drew, D. P. & Fincher, G. B. Gene structure and expression pattern analysis of three monodehydroascorbate reductase (Mdhar) genes in Physcomitrella patens: implications for the evolution of the MDHAR family in plants**. *Plant. Mol. Biol.* **60**, 259–275 (2006).
52. Leterrier, M., Corpas, F. J., Barroso, J. B. & Sandalio, L. M. Del Río, L. A. Peroxisomal monodehydroascorbate reductase. Genomic clone characterization and functional analysis under environmental stress conditions. *Plant. Physiol.* **138**, 2111–2123 (2005).
53. Sudan, J., Negi, B. & Arora, S. Oxidative stress induced expression of monodehydroascorbate reductase gene in Eleusine coracana. *Physiol. Mol. Biology Plants.* **21**, 551–558 (2015).
54. Beerling, D. J. & Berner, R. A. Impact of a Permo-Carboniferous high O2 event on the terrestrial carbon cycle. *Proceedings of the National Academy of Sciences* 97, 12428–12432 (2000).
55. Savard, L. et al. Chloroplast and nuclear gene sequences indicate late Pennsylvanian time for the last common ancestor of extant seed plants. *Proc. Natl. Acad. Sci.* **91**, 5163–5167 (1994).
56. Pang, Y., Hu, Y. & Bao, J. Comparative phosphoproteomic analysis reveals the response of starch metabolism to high-temperature stress in rice endosperm. *Int. J. Mol. Sci.* **22**, (2021).
57. Liu, X., Hu, B. & Chu, C. Nitrogen assimilation in plants: current status and future prospects. *J. Genet. Genomics.* **49**, 394–404 (2022).
58. Hauryliuk, V., Atkinson, G. C., Murakami, K. S., Tenson, T. & Gerdes, K. Recent functional insights into the role of (p)ppGpp in bacterial physiology. *Nat. Rev. Microbiol.* **13**, 298–309 (2015).
59. Sandhu, J. et al. Natural variation in LONELY GUY-Like 1 regulates rice grain weight under warmer night conditions. *Plant. Physiol.* **196**, 164–180 (2024).
60. Zeeman, S. C., Kossmann, J., Smith, A. M. & Starch Its metabolism, evolution, and biotechnological modification in plants. *Annu. Rev. Plant. Biol.* **61**, 209–234 (2010).
61. Aprile, A. et al. Different stress responsive strategies to drought and heat in two durum wheat cultivars with contrasting water use efficiency. *BMC Genom.* **14**, 821 (2013).
62. Fortunato, S., Lasorella, C., Dipierro, N., Vita, F. & de Pinto, M. C. Redox Signaling in Plant Heat Stress Response. *Antioxidants* 12, (2023).
63. Lou, G. et al. FLOURY ENDOSPERM19 encoding a class I glutamine amidotransferase affects grain quality in rice. *Mol. Breeding.* **41**, 36 (2021).
64. Dhatt, B. K. et al. Allelic variation in rice fertilization independent endosperm 1 contributes to grain width under high night temperature stress. *New Phytol.* **229**, 335–350 (2021).
65. Buell, C. R. Current status of the sequence of the rice genome and prospects for finishing the first monocot genome. *Plant. Physiol.* **130**, 1585–1586 (2002).
66. de Dal'Molin, O., Quek, C. G., Saa, L. E. & Nielsen, L. K. P. A. A multi-tissue genome-scale metabolic modeling framework for the analysis of whole plant systems. *Front. Plant. Sci.* **6**, (2015).

Acknowledgements

R.S. gratefully acknowledges funding support from the National Science Foundation (NSF) CAREER grant

(1943310). H.W. acknowledges National Institute of Food and Agriculture (NIFA) Award #2024-67013-42385. The authors declare no competing interests.

Author contributions

R.S. and H.W. designed the study and oversaw the project and funding acquisition; N.B.C. performed data curation, formal analysis, validation, and visualization; N.B.C. and A.N.C. worked on methodology; N.B.C. and A.N.C. wrote the original draft; R.S. and H.W. reviewed and edited the draft.

Declarations

Competing interest

The authors declare no competing interests.

Additional information

Supplementary Information The online version contains supplementary material available at https://doi.org/10.1038/s41598-025-00504-6.

Correspondence and requests for materials should be addressed to R.S.

Reprints and permissions information is available at www.nature.com/reprints.

Publisher's note Springer Nature remains neutral with regard to jurisdictional claims in published maps and institutional affiliations.